

# Spectrometry of the Earth using Neutrino Oscillations

C. Rott<sup>1</sup>, A. Taketa<sup>2</sup>, D. Bose<sup>1</sup>

<sup>1</sup>*Department of Physics, Sungkyunkwan University, Suwon 440-746, Korea.*

<sup>2</sup>*Earthquake Research Institute, University of Tokyo, 1-1-1 Yayoi, Bunkyo-ku, Tokyo, Japan.*

The unknown constituents of the interior of our home planet have provoked the human imagination and driven scientific exploration. We herein demonstrate that large neutrino detectors could be used in the near future to significantly improve our understanding of the Earth's inner chemical composition. Neutrinos, which are naturally produced in the atmosphere, traverse the Earth and undergo oscillations that depend on the Earth's electron density. The Earth's chemical composition can be determined by combining observations from large neutrino detectors with seismic measurements of the Earth's matter density. We present a method that will allow us to perform a measurement that can distinguish between composition models of the outer core. We show that the next-generation large-volume neutrino detectors can provide sufficient sensitivity to reject outer core models with large hydrogen content and thereby demonstrate the potential of this novel method. In the future, dedicated instruments could be capable of distinguishing between specific Earth composition models and thereby reshape our understanding of the inner Earth in previously unimagined ways.

---

Correspondence and requests for materials should be addressed to C.R. (email: rott@skku.edu) and A.T. (email: taketa@eri.u-tokyo.ac.jp). Order of first and second authors is determined by lot.

Understanding the inner structure and composition of the Earth is fundamental to Earth science. While Earth's matter density distribution can be inferred from geophysical observations, its compositional structure is far more difficult to determine. The state and composition of the core, which constitutes 32% of Earth's mass and 16% of its volume, remains largely uncertain. The core consists of an iron nickel alloy and is divided into inner and outer regions distinguished by a large density difference at a depth of approximately 5,100 km. The inner core is solid, while the lack of s-wave propagation in the outer core and lower density indicate it to be liquid. The density deficit in the outer core, however, cannot be simply explained by a difference in state, but rather requires the presence of light elements at 5 wt% to 10 wt%. There is great excitement in Earth science with regard to determining these light components in the outer core in order to understand the evolution of the Earth and the geodynamo. We introduce a new technique based on neutrino oscillations in order to remotely measure electron density and demonstrate how, in the near future, this method could be used to distinguish between different composition models of the inner Earth.

Analyses of seismic waves have resulted in the well-understood shell structure of the Earth, consisting of crust, upper mantle, lower mantle, outer core, and inner core. The matter density structure of the Earth has been accurately determined by combining astronomic-geodetic parameters, free oscillation frequencies, and seismic wave velocity measurements <sup>1</sup>. The composition of the crust near the surface can be measured directly. Drill core samples have resulted in composition measurements down to a depth of approximately 12 km <sup>2</sup>. The upper mantle composition can be probed through eruption entrainment sampling <sup>3</sup>. The state and composition of the Earth's core, at a depth of approximately 2,900 km remains far more uncertain with no prospects of sampling materials.

The outer core composition can be inferred to be mostly iron-nickel alloy with traces of light elements, by combining seismological velocity profiles and the composition of primitive meteorites <sup>4</sup>. Through recent progress in high-pressure experiments, hydrogen, carbon, oxygen, silicon, and sulfur have been suggested as light element candidates <sup>5</sup>. However, the abundance of these light elements remains uncertain.

Obtaining reliable estimates for the abundances of light elements in the Earth's core is essential to understanding the formation and evolution of the Earth <sup>6</sup> and to determining the origin of the geomagnetic field <sup>7</sup>, which are two of the major unsolved mysteries in Earth science.

Neutrinos (denoted  $\nu$ ) are remarkable particles that have enjoyed an ever more important role in particle physics, cosmology, and astrophysics since they were predicted by theorist Wolfgang Pauli in 1930 and first observed in 1956 <sup>8</sup>. There exist three different types (referred to as flavours) of neutrinos,  $\nu_e$ ,  $\nu_\mu$ , and  $\nu_\tau$ , which relate to how the neutrino was produced. However, a neutrino's flavour can change. For example, a neutrino produced as a  $\nu_\mu$  can be detected as a  $\nu_e$ . This process, which solved the solar neutrino problem <sup>9</sup>, is known as neutrino oscillation <sup>10</sup>. Neutrino oscillations are a quantum mechanical consequence of neutrinos having mass, and as such the behaviour of these oscillations can be described precisely.

In the present study, we propose a novel technique for measuring the average chemical composition of the deep Earth using neutrinos. Due to their tiny interaction cross section, neutrinos can pass through the entire Earth without interacting. As mentioned earlier, due to neutrino oscillations, a flavour of one neutrino can convert to another flavour. Neutrino oscillations depend on the medium traversed, or, more specifically, on the electron density along the path of the neutrino through the Earth <sup>11</sup>. The compositional structure of the Earth can be obtained as the average ratio of the atomic number to the atomic weight ( $Z/A$ ), by comparing the electron density distribution and the Earth's matter density distribution. This effect makes neutrinos unique messenger particles to remotely probe the Earth's interior.

Large-volume neutrino detectors have emerged as powerful tools in particle physics and astrophysics. Operating instruments have demonstrated their tremendous potential in groundbreaking discoveries, such as the observation of high-energy extra-terrestrial neutrinos by IceCube and through the observation of neutrino oscillations by Super-Kamiokande. There is a great interest in constructing the next generation of neutrino detectors with larger volumes and improved performance. This new generation of large-volume detectors could be capable of observing neutrinos at

sufficiently high rates to perform the first experimental measurement of the Earth's interior. For example, with the advent of Hyper-Kamiokande (Hyper-K) <sup>12</sup> and the Precision IceCube Next-Generation Upgrade (PINGU) <sup>13</sup>, spectrometry using neutrino oscillations could enable us to, for the first time, directly determine the compositional structure of the Earth. Even more visionary ideas, such as large ocean-going <sup>14</sup> or ice-based detectors, could see neutrino spectrometry emerge as a precision science.

Preceding research of geophysics using neutrinos can be divided into three categories: (1) measurement of the radioactive nuclei density in the Earth using geo-neutrinos generated through nuclear decays, (2) measurement of Earth's matter density using neutrino absorption, and (3) measurement of Earth's matter density using neutrino oscillations <sup>15-21</sup>. In the present study, we introduce a new fourth category. We apply neutrino oscillations for a composition measurement, exploiting the fact that neutrino oscillations are dependent on electron density, which is the product of the matter density and the ratio of the average atomic number to the atomic weight. Although the underlying physical phenomena are well understood, we focus in particular on the relevance of these effects to geophysics and discuss the prospects for an Earth composition measurement that could be performed within the next two decades.

## Results

**Neutrino oscillations in the Earth** In geophysics, neutrinos have received attention due to the information on the inner Earth they provide, as demonstrated by the measurement of radiogenic heat generated in the Earth through the observations of neutrinos from nuclear decays of uranium and thorium <sup>22</sup>. The success in detecting these geoneutrinos has confirmed the feasibility of using neutrinos in Earth science. While geoneutrinos are generated through nuclear decay and carry energies of approximately  $10^6$  eV (one electron volt (eV) =  $1.602 \times 10^{-19}$  joules), the neutrinos used for the proposed method have energies of a few GeV ( $10^9$  eV) and are naturally produced when energetic cosmic rays collide with the upper Earth's atmosphere.

The majority of atmospheric neutrinos produced are type  $\nu_\mu$ , and their flavour changes as they pass straight through the Earth. The neutrino oscillation probability depends on a set of oscillation parameters, the neutrino energy,  $E_\nu$ , the distance travelled, and the electron density along its path. The path length,  $L$ , is the distance that the neutrino travels from its point of origin in the atmosphere to the detector. Since all neutrinos relevant for this analysis are generated in the Earth's atmosphere,  $L$  is simply a function of the zenith angle,  $\Theta$ , of the neutrino arrival direction at the detector. Figure 1(a) shows the neutrino path through the Earth.

We calculate neutrino oscillation probabilities, following the approach of Barger et al.<sup>11</sup> and use the numerical implementation of the NuCraft software package<sup>23</sup>. The oscillation parameters, which are well measured, are taken from the global fit given by Capozzi et al.<sup>24</sup>, assuming the case of a normal mass hierarchy, as favoured in current measurements. We use the modified Preliminary Reference Earth Model (PREM) matter density model<sup>1,25</sup> to describe the Earth density and structure. We fix the mantle composition to pyrolite and the inner core composition to iron, only the outer core composition is varied. Figure 1(b) shows the  $\nu_\mu$  survival probability and the  $\nu_e$  appearance probability as a function of the path length for a neutrino with an energy of 4 GeV ( $10^9$  eV) passing vertically through the Earth. The survival probability is the probability that a created neutrino of specific flavour is observed as such. In this case, we consider a muon neutrino observed as such  $P(\nu_\mu \rightarrow \nu_\mu)$ . The appearance probability is the chance that a neutrino of one flavour is observed as a neutrino of a different flavour, for example  $P(\nu_\mu \rightarrow \nu_e)$ . The flavour change as a function of travelled distance in the Earth is shown. In order to visually show the impact of the outer core composition on the oscillation probability, we compare the cases of an alloy of iron and 2 wt% (weight percent) hydrogen with iron. Figure 1(c) shows the  $\nu_\mu$  survival probability at the surface of the Earth, as a function of the neutrino's energy for four different core compositions. In order to visualize the difference in survival probability for different outer core compositions, we selected (1) iron, (2) an alloy of iron and 1 wt% hydrogen, (3) an alloy of iron and 2 wt% hydrogen, and (4) an alloy of iron and 5 wt% hydrogen as extreme examples of the outer core composition.

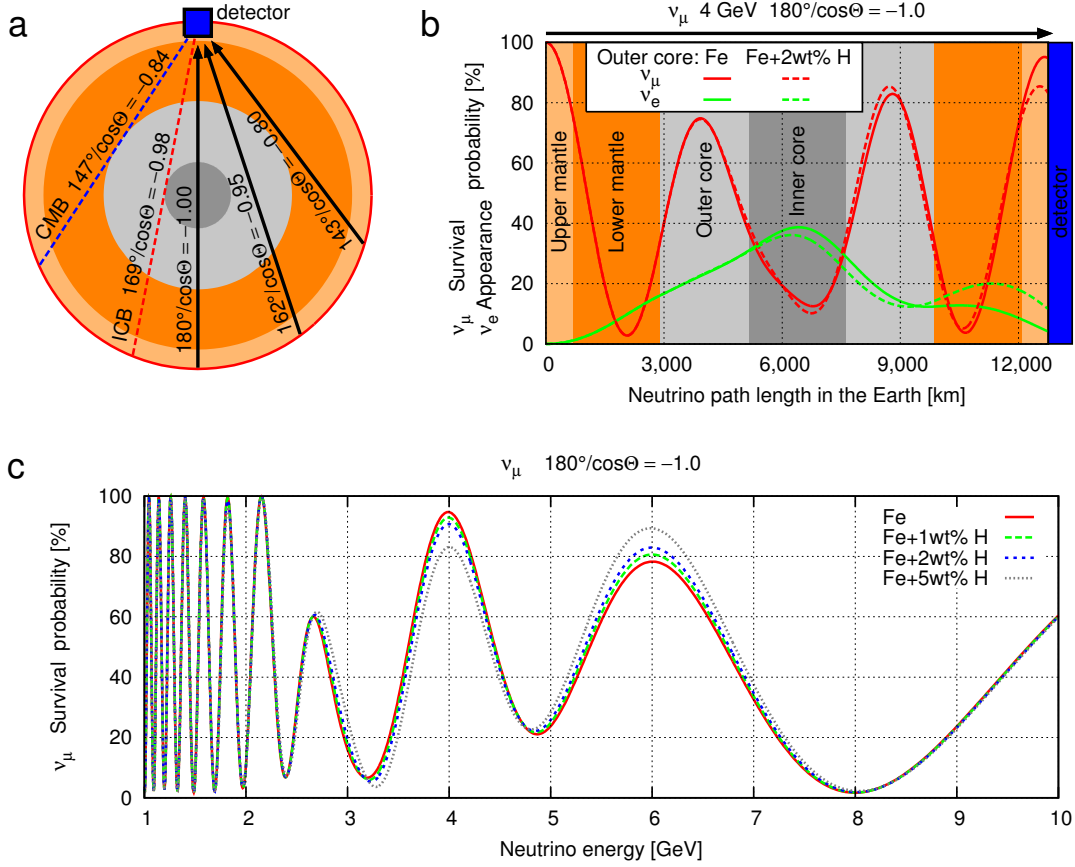


Figure 1: (a) Schematic diagram of a neutrino's path through the Earth and the corresponding zenith angles. The inner core boundary (ICB) at  $\Theta = 169^\circ$  and the core mantle boundary (CMB) at  $\Theta = 147^\circ$  are indicated by dashed red and blue lines, respectively. (b)  $\nu_e$  appearance probability (green) and  $\nu_\mu$  survival probability (red) as functions of path length in the Earth. The neutrino direction is  $\Theta = 180^\circ$ , as shown in (a). The solid/dashed line corresponds to the case in which the composition of the outer core is pure iron/an alloy of iron and 2 wt% hydrogen. (c)  $\Theta = 180^\circ - \nu_\mu$  survival probabilities as a function of neutrino energy for different outer core compositions. The solid (red), long dashed (green), short dashed (blue), and dotted (gray) lines represent iron, an alloy of iron and 1 wt% hydrogen, an alloy of iron and 2 wt% hydrogen, and an alloy of iron and 5 wt% hydrogen, respectively.

**Z/A ratios for different outer core models** Iron is the most abundant element in the outer Earth core and throughout this document we have chosen pure iron as our default composition. Models adding single or multiple elements to iron have been proposed <sup>26–28</sup>. In Table 1, we introduce some selected outer core composition models and characterize them according to Z/A ratio. The estimated maximal abundance of light elements <sup>5,29</sup> for alloys of iron are listed in Table 1. Note that nickel is thought to co-exist with iron in the outer core, with an estimated content of approximately 5% <sup>30</sup>. Since there is only a slight difference between Z/A values, using an alloy of iron and 5 wt% nickel as the base composition rather than iron will result in only a marginal change in Z/A from 0.4656 to 0.4661.

Table 1: Z/A ratios for alloys of iron and light elements and some selected composition models.

| Model name                                     | Z/A ratio | Si(wt%) | O(wt%) | S(wt%) | C(wt%) | H(wt%) | reference                    |
|--|-----------|---------|--------|--------|--------|--------|------------------------------|
| Single-light-element model (maximum abundance) |           |         |        |        |        |        |                              |
| Fe+18wt%Si                                     | 0.4715    | 18      | -      | -      | -      | -      | Poirier <sup>29</sup>        |
| Fe+11wt%O                                      | 0.4693    | -       | 11     | -      | -      | -      | Poirier <sup>29</sup>        |
| Fe+13wt%S                                      | 0.4699    | -       | -      | 13     | -      | -      | Li and Fei <sup>5</sup>      |
| Fe+12wt%C                                      | 0.4697    | -       | -      | -      | 12     | -      | Li and Fei <sup>5</sup>      |
| Fe+1wt%H                                       | 0.4709    | -       | -      | -      | -      | 1      | Li and Fei <sup>5</sup>      |
| Multiple-light-element model                   |           |         |        |        |        |        |                              |
| Allegre2001                                    | 0.4699    | 7       | 5      | 1.21   | -      | -      | Allègre et al. <sup>26</sup> |
| McDonough2003                                  | 0.4682    | 6       | 0      | 1.9    | 0.2    | 0.06   | McDonough <sup>27</sup>      |
| Huang2011                                      | 0.4678    | -       | 0.1    | 5.7    | -      | -      | Huang et al. <sup>28</sup>   |

**Oscillation probabilities for different outer core models** As neutrino oscillations simply depend on the neutrino’s energy, path length, and composition along the path, we can determine the probability that a neutrino will change flavours as a function of the zenith angle and the energy. We calculated the oscillation probabilities for different core models. Figure 2 shows such an oscillogram, i.e., oscillation probabilities as a function of zenith angle and neutrino energy, for two different outer core compositions. Subtle differences in the neutrino survival probability can be

exploited in order to distinguish between different composition models. The most pronounced differences in survival probability are for neutrinos with energies between 2 GeV and 8 GeV that traverse the outer core, i.e., their zenith angles are larger than  $147^\circ$ .

**Detector requirements** The described differences in neutrino oscillation effects that depend on the Earth's composition could be detectable with a neutrino detector if the detector combines good energy and angular resolution in the relevant energy range and observes GeV neutrinos at sufficiently high rates to accumulate sufficient statistical samples. Due to the small neutrino interaction cross section, a large detector volume of megaton scale is necessary in order to acquire a sufficient number of neutrino events and not suffer from limited statistics. Good neutrino flavour identification can be beneficial.

**Neutrino detectors** Large neutrino detectors have been realized in a cost-effective manner by using water or ice as a naturally occurring detector medium to observe Cherenkov light emissions from one or more energetic particles produced in neutrino interactions. The IceCube neutrino telescope<sup>31</sup> uses one gigaton (1,000 megatons) of ice at the Geographic South Pole that was instrumented with more than 5,000 photosensors. The optical sensor array relies on the ultra-pure Antarctic ice as a detection medium. The detector is working extremely well, and the recent discovery of high-energy astrophysical neutrinos demonstrates the potential of large neutrino detectors<sup>32</sup>. Super-Kamiokande<sup>33</sup>, which is the leading high-precision detectors, has a 50 kiloton water tank surrounded by 11,000 photosensors to observe Cherenkov light, allowing neutrino energies to be determined with high precision and neutrino flavours to be identified reliably. The underlying technology applied by IceCube and Super-Kamiokande is well established and is the basis for future detectors. Next-generation detectors could benefit from better photosensors with higher photon detection efficiency.

**Sensitivity of benchmark detectors** We calculate the confidence level with which the composition of the outer core could be determined for some benchmark neutrino detectors. We use a generic neutrino detector description based on performance parameters to estimate sensitivities.

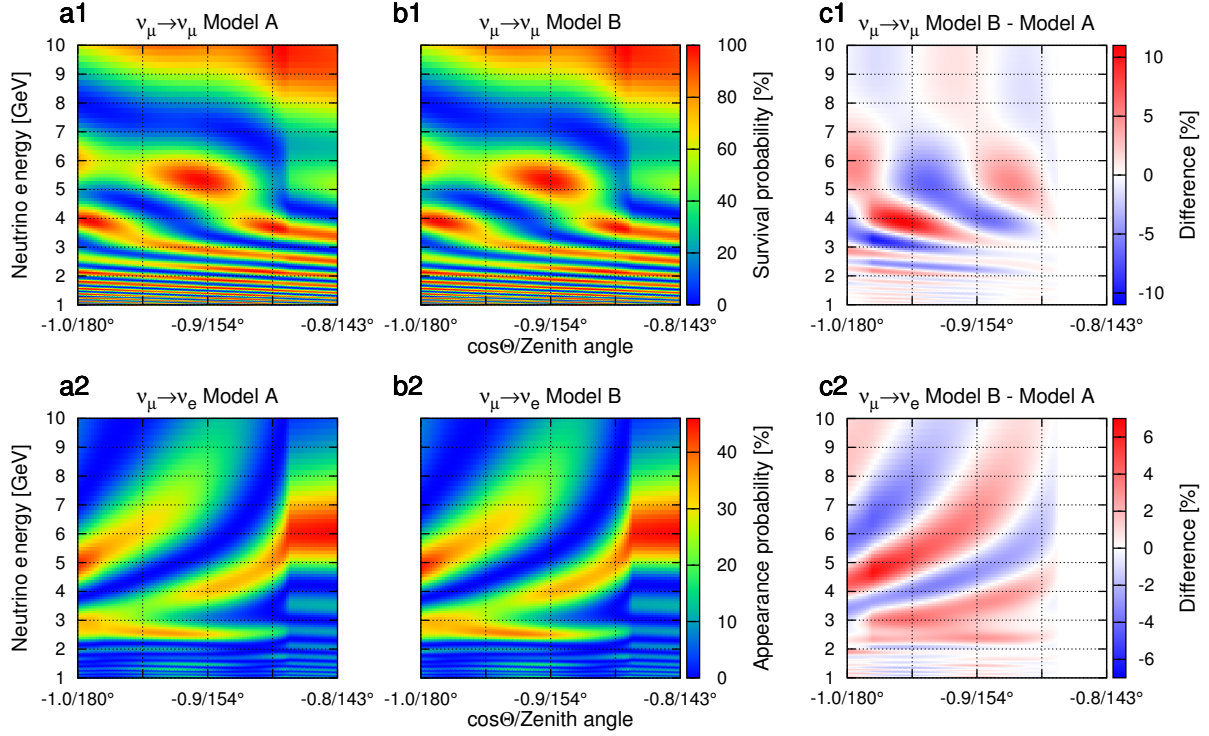


Figure 2: Comparison of oscillation probabilities for two different core compositions: Model A – iron; Model B – an alloy of iron and 2 wt% hydrogen. a1 and a2 show the  $\nu_\mu$  survival probabilities as a function of neutrino energy and zenith angle for Models A and B, respectively. b1 and b2 show the appearance probability for  $\nu_\mu$  to  $\nu_e$  for Models A and B, respectively. a3 shows the difference between a1 and a2, and b3 shows the difference between b1 and b2.

Our parameterization can easily be converted into hardware and design requirements for the planning of new detectors. We compute expected event rates as a function of the neutrino energy and the zenith angle as a function of the product of detector size and the exposure time in megaton-years. In this way, we calculate the number of neutrino events for a certain energy, direction, and flavour. We create templates of the expected event rates for different outer core models. Event rates were calculated from the atmospheric neutrino flux, oscillation probabilities, neutrino cross section, detector volume, and exposure time. The atmospheric neutrino flux and energy spectrum are well understood for our purposes. We adopt the atmospheric neutrino flux model of Athar et al. <sup>34</sup>. For the neutrino ( $\nu_\mu$ ) and anti-neutrino ( $\bar{\nu}_\mu$ ) interaction cross sections, we use the approximate values of  $7.0 \times (E/\text{GeV}) \times 10^{-39} \text{cm}^2$  and  $3.0 \times (E/\text{GeV}) \times 10^{-39} \text{cm}^2$ , respectively <sup>35</sup>.

The outcome of any experimental measurement that deals with individual events, such as the detection of neutrinos, will be subject to statistical fluctuations. We consider a large number of potential experimental outcomes, called pseudo experiments, in order to estimate the chance that models could be distinguished through an actual measurement. For each pseudo experiment, we compare the number of observed events to the number of expected events for a specific model. We calculate events for given ranges of energy and zenith angle. For each of these bins in energy and zenith angle, events follow Poisson statistics and we determine the probability for the observation. We then compute the likelihood of this experimental outcome with respect to a specific Earth model assumption. The total likelihood is then given by the product of the likelihoods for the individual bins. In order to compare the likelihood of one model with that of another, we compute the likelihood ratio. For the calculation of the expected significance, we perform a set of pseudo experiments and apply the log-likelihood ratio (LLR) method <sup>36</sup>.

For simplicity of the analysis, we consider only muon neutrino ( $\nu_\mu + \bar{\nu}_\mu$ ) events, which are the most relevant for neutrino spectrometry. Muon neutrino events can be identified with high efficiency by proposed next-generation detectors, such as PINGU or Hyper-K. For PINGU, the resolution for the muon neutrino energy is expected to be better than 25% at 5 GeV, and the zenith angle resolution for the neutrino has been reported to be approximately  $13^\circ$  <sup>13</sup>. At Hyper-K, better

angular and energy resolutions compared to PINGU can be expected, in addition to a larger than 99% efficiency to identify the interaction products of a neutrino interaction <sup>12,37</sup>.

Figure 3 shows the sensitivity for rejecting outer core compositions given by their  $Z/A$  ratios with respect to iron for a generic neutrino detector. The detector is characterized by energy resolution and angular resolution, as defined by  $\Delta E_\nu/E_\nu = \alpha$  and  $\Delta\Theta = \beta/\sqrt{E/GeV}$ , respectively. We choose  $\alpha = 0.20$  and  $\beta = 0.25$  for our default benchmark detector and show the sensitivity depending on the product of lifetime and detector volume (megaton-years) in Figure 3(b). With an acquired dataset of 10 megaton-years, a neutrino detector could for the first time confirm an iron-like core through experimental measurements. Outer core compositions dominated by lead or water could be rejected with more than 99% confidence with respect to iron. The  $Z/A$  ratios of iron, lead, mantle (pyrolite), and water are 0.4656, 0.3958, 0.4957, and 0.5556, respectively. The large hydrogen content appearing at the axis at the top of each plot could be rejected. Figure 3(a) shows the prospects of neutrino spectrometry. A one-gigaton-year (or 1,000 megaton-year) dataset, which is equivalent to observation for 20 year using a 50 megaton detector, would provide the ability to discriminate between established outer core composition models. Furthermore, the hydrogen content of the outer core could be measured with a precision of 0.4 wt%. Better sensitivities could be achieved if the detector exceeds the benchmark detector performance parameters selected for use in the present study. Figures 3(c) and 3(d) show the energy resolution and angular resolution dependences of the sensitivity, respectively.

Note that neutrino spectrometry itself only determines the  $Z/A$  ratio; hence, the resulting measurement could be degenerate in corresponding Earth composition models. A model with Fe (90 wt%)+O (10 wt%) ( $Z/A=0.4690$ ) could be clearly distinguished from an iron core ( $Z/A = 0.4656$ ), but would have a relatively similar signature as a model with Fe (90 wt%) + Ni (5 wt%) + Si (5 wt%) ( $Z/A=0.4681$ ). Since oxygen, sulfur, silicon, and carbon have relatively similar  $Z/A$  ratios, neutrino spectrometry would be accompanied by ambiguities in the measurement of these elements. High-pressure experiments <sup>38</sup> combined with neutrino spectrometry could resolve the remaining degeneracies to allow estimation of the relative abundances of light elements.

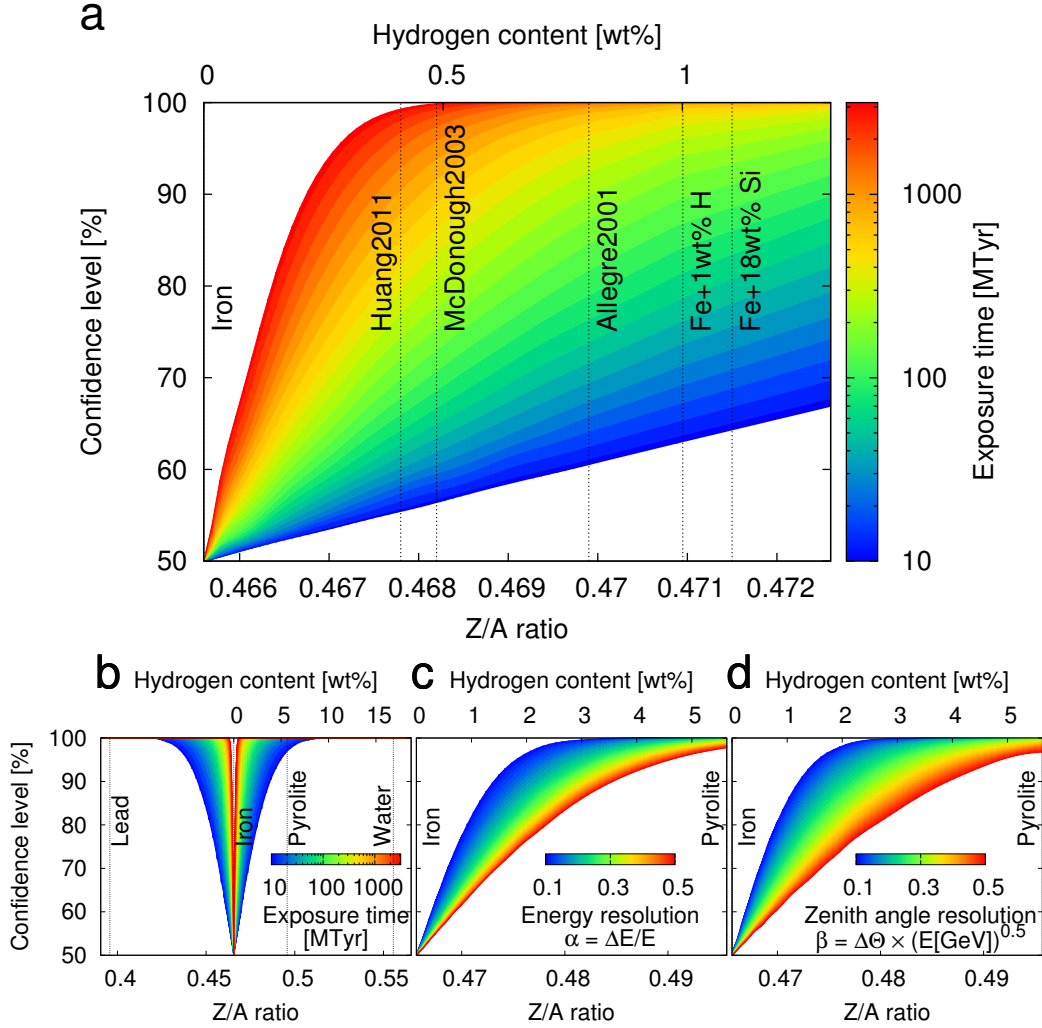


Figure 3: (a) Expected confidence level for rejecting a specific outer core composition with respect to iron plotted as a function of the corresponding  $Z/A$  ratio. A generic detector case with an energy resolution of 20% and an angular resolution of  $0.25 \times (E/\text{GeV})^{-0.5}$  is shown as an example. The colour indicates the exposure time given in megaton-years. We indicate the  $Z/A$  ratios for some selected outer core composition models (see Table 1 for details) as black dotted vertical lines. (b) The same plot as (a) for a larger  $Z/A$  range. Sensitivity dependences on (c) energy resolution and (d) angular resolution for a generic detector with an exposure time of 30 megaton-years for an angular resolution of  $0.25 \times (E/\text{GeV})^{-0.5}$  and an energy resolution of 20%, respectively.

**Uncertainties** We examine our results and the feasibility of the neutrino spectrometry measurement with future neutrino detectors with respect to theoretical and experimental uncertainties.

Uncertainties in the composition measurement originate from limited knowledge of the neutrino oscillation parameters, atmospheric neutrino flux uncertainties, neutrino cross-section uncertainties, and uncertainties in the Earth’s matter density profile. In addition to these theoretical uncertainties, detector acceptance-related uncertainties must be determined. However, this is beyond the scope of the present study and would have to be carried out through experimental collaborations.

At present, the limited knowledge of neutrino mixing parameters is the major source of uncertainty in the proposed neutrino spectrometry measurement. Using the current best-fit oscillation parameters and their uncertainty<sup>24</sup>, the error in the confidence level curve was approximately  $\pm 4\%$  at 90% (see Supplementary Figure 1). Several experiments are planned for the near future in order to realize more precise measurements of the neutrino mixing parameters<sup>39–41</sup>. A better determination of the neutrino oscillation parameters will reduce uncertainties.

In order to estimate the uncertainty resulting from the matter density models, we calculated the confidence level curves using three different density models (PREM500<sup>1,25</sup>, AK135<sup>42</sup>, PEM-A<sup>43</sup>; see Supplementary Figure 2). The systematic error resulting from the matter density in the confidence level curve was negligible compared with the systematic error resulting from the mixing parameters (see Supplementary Figure 3). The expected uncertainty is sufficiently small to distinguish the models introduced in the present study. However, in order to determine the light material contents in the outer core, a more precise mixing parameter and matter density model, which may be available in the near future, are needed.

The uncertainty in the atmospheric neutrino flux is estimated to be approximately 10%<sup>34,44</sup>. However, this uncertainty does not directly affect the Earth composition measurement, because the atmospheric neutrino flux can be measured by the neutrino detector itself. The flux ratio ( $\nu_\mu +$

$\bar{\nu}_\mu)/(\nu_e + \bar{\nu}_e)$ , on the other hand, may be affected if the detector cannot reliably provide a particle identification to distinguish between  $\nu_e$  and  $\nu_\mu$  events. Since the downward-moving neutrino flux is not subject to oscillations (due to the short distance), it can be used to measure the flavour ratio using the detector itself.

At present, the neutrino mass hierarchy, one of the remaining fundamental neutrino properties, is unknown. By the time that the proposed composition measurement is performed, we can safely assume that the mass hierarchy will have been determined, potentially even at the same neutrino detector considered for our measurement<sup>45,46</sup>. A normal mass hierarchy will increase neutrino oscillation probabilities and thus make neutrino spectroscopy measurements easier. A normal mass hierarchy is currently favoured<sup>47</sup> in global fits and is therefore used in the present study. If the mass hierarchy turns out to be inverted, the expected neutrino oscillation probabilities at the neutrino detector will be reduced, and in order to obtain the same sensitivity as in the normal hierarchy case, a detector would have to acquire a dataset that is six times larger.

## Discussions

Neutrino oscillations provide a way to distinguish different Earth composition models by probing the  $Z/A$  ratio. We expect neutrino spectroscopy to develop into a unique method for measuring the chemical composition of the inner Earth, which will lead us to a better understanding of the Earth's evolution and the origin of the geomagnetic field. Large-volume neutrino detectors that can accumulate atmospheric neutrino samples at significant rates and have good angular and energy resolutions at neutrino energies of 2-8 GeV are needed for these measurements. In the future, new neutrino telescopes and upgrades to existing instruments will significantly enhance neutrino detection capabilities in the most relevant energy range for the spectroscopic measurement discussed here. The Hyper-K project will see the construction of a 0.6-megaton fiducial volume detector comprising eight compartments and approximately 100,000 photosensors. PINGU will use a few megatons of ice in the centre of the IceCube detector where the ice is clearest. A detector of similar size is also considered as a deep-sea neutrino telescope in the Mediterranean Sea as part of

the KM3NeT project<sup>48,49</sup>. These next-generation neutrino detectors could already offer sufficient sensitivity in order to exclude extreme models of the Earth’s composition. If they are carefully optimized for neutrino spectrometry, the first meaningful bounds on the hydrogen content in the core could be in reach. In the future, dedicated neutrino experiments could be used to distinguish between different composition models, as we have demonstrated. We limited our research to a conservative scenario considering that only muon neutrinos are detected. The detection of neutrinos of different flavours is expected to enhance the sensitivity of the proposed method, warranting further investigation in the future.

In the present study, we focused on the composition of the outer core, but neutrino spectrometry could also be applied to the mantle, especially in order to elucidate the water content of the lower mantle. Through recent progress in diamond inclusion sampling, high-pressure experiments, and dense seismic velocity measurements, it was found that the uppermost part of the lower mantle can reserve 1 wt% water<sup>50</sup>. Neutrino spectrometry has the ability to provide an upper limit for the water content of the lower mantle in the same way as the hydrogen content of the outer core.

## Methods

**Flux calculation** Event distributions for a generic neutrino detector defined by volume, energy resolution, and angular resolution were calculated for angle-averaged atmospheric neutrino fluxes after propagation through the Earth. The calculation proceeded in two steps. We first calculated the transition probabilities for neutrinos of all flavours as function of zenith angle and energy. The results were binned in 720 bins of the cosine of zenith angle and 400 bins of energy to form a transfer matrix  $M$ . Full three-flavour neutrino oscillations were performed, and an Earth structural model with 400 layers (see Supplementary Figure 2) and various composition models was used. The predicted neutrino flux for muon neutrinos obtained from the Honda model was propagated through the Earth using transition tables describing the muon neutrino survival probability and binned in 40 bins of the log of reconstructed neutrino energy and in 20 bins of the cosine of the reconstructed zenith angle for the range of  $\cos\Theta = (-1\dots 0)$  and  $\log(E)=0\dots 1$ . The reconstructed

zenith angle and neutrino energies were randomly sampled from the expected distribution as defined by the detector model (assuming Gaussian distributions). For each bin of  $M$ , 100,000 events were generated and mapped into the reconstruction matrix, weighted by the expected Honda flux. Rates were calculated according to the neutrino interaction cross section and the product of the detector volume and operation time (megaton-years). Each bin  $m_{ij}$  of  $M$  obtains the expectation value of an observation, were a measurement to be performed. Using a different Earth composition model and the same generic detector model, we can obtain the expectation values for this model  $m_{ij}^*$ . Here,  $m_{ij}$  and  $m_{ij}^*$  act as templates for our log-likelihood analysis in order to determine the model sensitivity.

**Log-likelihood method** Ensembles of pseudo datasets are drawn from each template  $m_{ij}^*$  and  $m_{ij}$  that are repeatedly varied following Poisson statistics. The log of the Poisson likelihood of the pseudo data for a specific bin is calculated with respect to the corresponding bin in  $m_{ij}^*$  and  $m_{ij}$ . We take the sum of  $(-2) \log(P(o_{ij}, m_{ij}))$  to obtain the total likelihood. In this way, for each pseudo dataset, two likelihoods are calculated and are labelled  $\mathcal{L}(\text{pseudo data, template})$ . The likelihoods are used to calculate LLR. We calculate two distributions for pseudo data  $o_{ij}$  drawn from  $m_{ij}$  given by  $\mathcal{L}(o(m)|m) / \mathcal{L}(o(m)|m^*)$  and  $\mathcal{L}(o(m^*)|m) / \mathcal{L}(o(m^*)|m^*)$ . A total of 10,000 pseudo datasets are used to achieve adequate coverage of the probability space. We obtain expected significances from our ensemble of pseudo experiments. The probability of distinguishing model  $m$  from  $m^*$  is obtained by calculating the fraction of cases in which events drawn from  $m$  have a likelihood ratio that is more consistent with  $m$  than  $m^*$ .

1. Dziewonski, A. & Anderson, D. Preliminary reference Earth model. *Physics of the Earth and Planetary Interiors* **25**, 297–356 (1981).
2. Popov, Y., Pevzner, S., Pimenov, V. & Romushkevich, R. New geothermal data from the Kola superdeep well SG-3. *Tectonophysics* **306**, 345–366 (1999).
3. Hofmann, A. W. Mantle geochemistry: the message from oceanic volcanism. *Nature* **385**, 219–229 (1997).

4. McDonough, W. & Sun, S. The composition of the Earth. *Chemical Geology* **120**, 223–253 (1995).
5. Li, J. & Fei, Y. Experimental Constraints on Core Composition. In Carlson, R. W. (ed.) *Treatise on geochemistry*, vol. 2, chap. 2.14 (Elsevier, Amsterdam, 2007).
6. Allègre, C. J., Poirier, J., Humler, E. & Hofmann, A. W. The chemical composition of the Earth. *Earth and Planetary Science Letters* **134**, 515–526 (1995).
7. Fearn, D. R. & Loper, D. E. Compositional convection and stratification of Earth’s core. *Nature* **289**, 393–394 (1981).
8. Cowan, C. L., Reines, F., Harrison, F. B., Kruse, H. W. & McGuire, A. D. Detection of the Free Neutrino: a Confirmation. *Science (New York, N.Y.)* **124**, 103–4 (1956).
9. Bahcall, J. N. & Pinsonneault, M. H. Standard solar models, with and without helium diffusion, and the solar neutrino problem. *Rev. Mod. Phys.* **64**, 885–926 (1992).
10. Pontecorvo, B. Mesonium and anti-mesonium. *Sov.Phys.JETP* **6**, 429 (1957).
11. Barger, V., Whisnant, K., Pakvasa, S. & Phillips, R. Matter effects on three-neutrino oscillations. *Physical Review D* **22**, 2718–2726 (1980).
12. Abe, K. *et al.* Letter of Intent: The Hyper-Kamiokande Experiment — Detector Design and Physics Potential —. Preprint arXiv:1109.3262 (2011).
13. The IceCube-PINGU Collaboration. Letter of Intent: The Precision IceCube Next Generation Upgrade (PINGU). Preprint arXiv:1401.2046 (2014).
14. Kistler, M. D., Yüksel, H., Ando, S., Beacom, J. F. & Suzuki, Y. Core-collapse astrophysics with a five-megaton neutrino detector. *Physical Review D - Particles, Fields, Gravitation and Cosmology* **83**, 1–11 (2011).
15. Jacobsson, B., Ohlsson, T., Snellman, H. & Winter, W. The Effects of matter density uncertainties on neutrino oscillations in the earth. *J.Phys.* **G29**, 1873–1876 (2003).

16. Lindner, M., Ohlsson, T., Tomas, R. & Winter, W. Tomography of the Earth's core using supernova neutrinos. *Astroparticle Physics* **19**, 755–770 (2003).
17. Geller, R. J. & Hara, T. Geophysical aspects of very long baseline neutrino experiments. *Nuclear Instruments and Methods in Physics Research Section A: Accelerators, Spectrometers, Detectors and Associated Equipment* **503**, 187–191 (2003).
18. Winter, W. Probing the absolute density of the Earth's core using a vertical neutrino beam. *Physical Review D* **72**, 037302 (2005).
19. Winter, W. Neutrino tomography: Learning about the earth's interior using the propagation of neutrinos. *Earth Moon Planets* **99**, 285–307 (2006).
20. Gonzalez-Garcia, M., Halzen, F., Maltoni, M. & Tanaka, H. Radiography of Earth's Core and Mantle with Atmospheric Neutrinos. *Physical Review Letters* **100**, 061802 (2008).
21. Agarwalla, S. K., Li, T, Mena, O. & Palomares-Ruiz, S. Exploring the Earth matter effect with atmospheric neutrinos in ice. Preprint arXiv:1212.2238 (2012).
22. Araki, T. *et al.* Experimental investigation of geologically produced antineutrinos with KamLAND. *Nature* **436**, 499–503 (2005).
23. Wallraff, M. & Wiebusch, C. Calculation of oscillation probabilities of atmospheric neutrinos using nuCraft. Preprint arXiv:1409.1387 (2014).
24. Capozzi, F. *et al.* Status of three-neutrino oscillation parameters, circa 2013. *Physical Review D* **89**, 093018 (2014).
25. Durek, J. & Ekström, G. A radial model of anelasticity consistent with long-period surface-wave attenuation. *Bulletin of the Seismological Society of America* **86**, 144–158 (1996).
26. Allègre, C., Manhès, G. & Lewin, E. Chemical composition of the Earth and the volatility control on planetary genetics. *Earth. Planet. Sci. Lett.* **185**, 49–69 (2001).

27. McDonough, W. F. Compositional Model for the Earth's Core. *Treatise On Geochemistry* 547–568 (2003).
28. Huang, H. *et al.* Evidence for an oxygen-depleted liquid outer core of the Earth. *Nature* **479**, 513–6 (2011).
29. Poirier, J.-P. & Shankland, T. J. Dislocation melting of iron and the temperature of the inner core boundary, revisited. *Geophys. J. Int.* **115**, 147–151 (1993).
30. Wood, B. J., Walter, M. J. & Wade, J. Accretion of the Earth and segregation of its core. *Nature* **441**, 825–833 (2006).
31. Ahrens, J. *et al.* Sensitivity of the IceCube detector to astrophysical sources of high energy muon neutrinos. *Astroparticle Physics* **20**, 507–532 (2004).
32. Aartsen, M. G. *et al.* Evidence for high-energy extraterrestrial neutrinos at the IceCube detector. *Science (New York, N.Y.)* **342**, 1242856 (2013).
33. Fukuda, Y. *et al.* Measurement of a small atmospheric  $\nu_\mu/\nu_e$  ratio. *Physics Letters B* **433**, 9–18 (1998).
34. Sajjad Athar, M., Honda, M., Kajita, T., Kasahara, K. & Midorikawa, S. Atmospheric neutrino flux at INO, South Pole and Pyhäsalmi. *Physics Letters B* **718**, 1375–1380 (2013).
35. Formaggio, J. A. & Zeller, G. P. From eV to EeV: Neutrino cross sections across energy scales. *Reviews of Modern Physics* **84**, 1307–1341 (2012).
36. James, F. *Statistical methods in experimental physics*, vol. 7 (World Scientific Singapore, 2006).
37. Abe, K. *et al.* A Long Baseline Neutrino Oscillation Experiment Using J-PARC Neutrino Beam and Hyper-Kamiokande. Preprint arXiv:1412.4673 (2014).
38. Hirose, K., Labrosse, S. & Hernlund, J. Composition and State of the Core. *Annual Review of Earth and Planetary Sciences* **41**, 657–691 (2013).

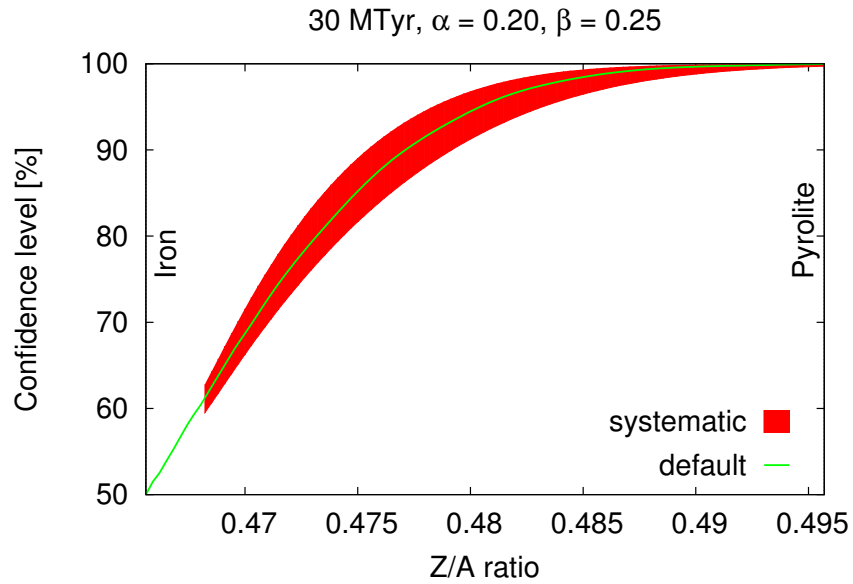
39. Abe, K. *et al.* The T2K experiment. *Nuclear Instruments and Methods in Physics Research Section A: Accelerators, Spectrometers, Detectors and Associated Equipment* **659**, 106–135 (2011).
40. An, F. P. *et al.* Observation of Electron-Antineutrino Disappearance at Daya Bay. *Physical Review Letters* **108**, 171803 (2012).
41. Li, Y. F. Overview of the Jiangmen Underground Neutrino Observatory (JUNO). Preprint arXiv:1402.6143. *arXiv preprint hep-ex/0701029* 4 (2014).
42. Kennett, B., Engdahl, E. & Buland, R. Constraints on seismic velocities in the earth from traveltimes. *Geophysical Journal International* **122**, 108–124 (1995).
43. Dziewonski, A., Hales, A. & Lapwood, E. Parametrically simple earth models consistent with geophysical data. *Physics of the Earth and Planetary Interiors* **10**, 12–48 (1975).
44. Honda, M., Kajita, T., Kasahara, K. & Midorikawa, S. Improvement of low energy atmospheric neutrino flux calculation using the JAM nuclear interaction model. *Physical Review D* 1–46 (2011).
45. Akhmedov, E. K., Razaque, S. & Smirnov, A. Y. Mass hierarchy, 2-3 mixing and CP-phase with Huge Atmospheric Neutrino Detectors. *JHEP* **1302**, 082 (2013).
46. Ge, S.-F., Hagiwara, K. & Rott, C. A Novel Approach to Study Atmospheric Neutrino Oscillation. *JHEP* **1406**, 150 (2014).
47. Fogli, G. L. *et al.* Global analysis of neutrino masses, mixings, and phases: Entering the era of leptonic CP violation searches. *Physical Review D - Particles, Fields, Gravitation and Cosmology* **86**, 1–11 (2012).
48. Katz, U. Status of the km<sup>3</sup>net project. *Nuclear Instruments and Methods in Physics Research Section A: Accelerators, Spectrometers, Detectors and Associated Equipment* **602**, 40–46 (2009).

49. Katz, U. for the KM3NeT Collaboration. The ORCA Option for KM3NeT. Preprint arXiv:1402.1022 (2014).
50. Schmandt, B., Jacobsen, S. D., Becker, T. W., Liu, Z. & Dueker, K. G. Dehydration melting at the top of the lower mantle. *Science* **344**, 1265–1268 (2014).

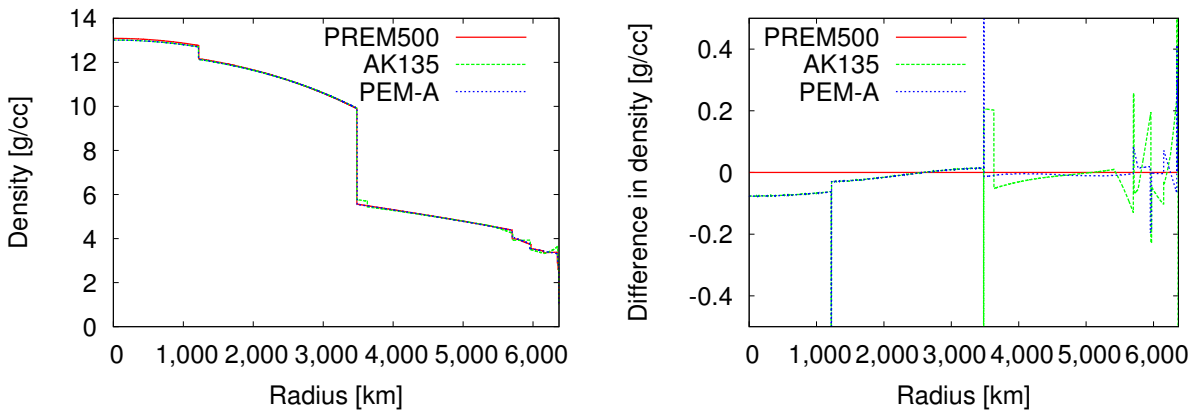
## **Acknowledgments**

We would like to thank William McDonough, Kotoyo Hoshina, and Hiroyuki Tanaka for engaging in useful discussions. The present study was supported by the Faculty Research Fund, Sungkyunkwan University, 2013. We used the computer systems of the Earthquake and Volcano Information Center of the Earthquake Research Institute, University of Tokyo.

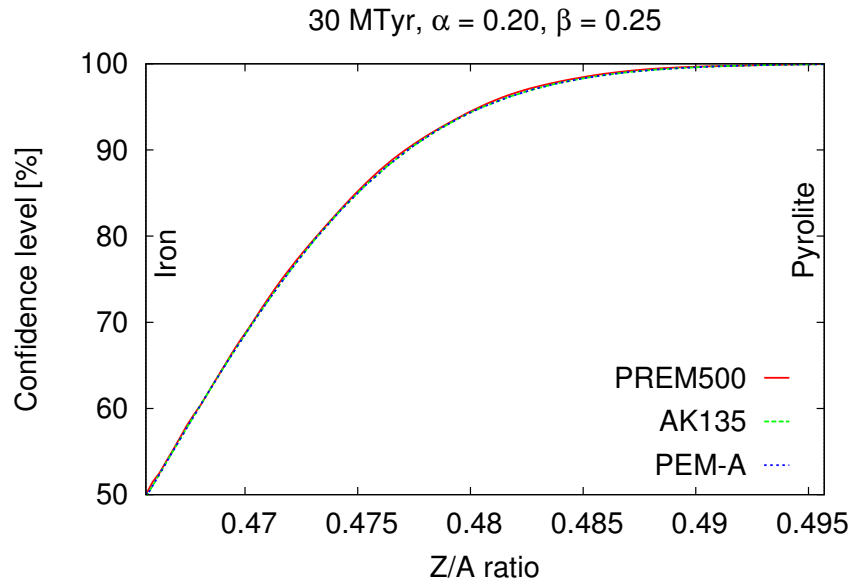
## **Supplementary Figures**



Supplementary Figure 1: Systematic error of the expected confidence level as a function of  $Z/A$ . The dashed (green) line represents default mixing parameter case and the red area represents its uncertainty. A generic detector case with an exposure time of 30 MTyr, an energy resolution of 20%, and an angular resolution of  $0.25 \times (E/\text{GeV})^{-0.5}$  is shown.



Supplementary Figure 2: left: Matter density distributions of the Earth as a function of radius from the centre of the Earth. The solid (red), dashed (green), and dotted (blue) lines represent the modified PREM, AK135, and PEM-A, respectively. right: Difference from modified PREM (PREM500).



Supplementary Figure 3: Expected confidence level for rejecting a specific outer core composition with respect to iron plotted as a function of the corresponding  $Z/A$  ratio. A generic detector case with an exposure time of 30 MTyr, an energy resolution of 20%, and an angular resolution of  $0.25 \times (E/\text{GeV})^{-0.5}$  is shown. We estimated the confidence level using three different density models. The solid (red), dashed (green), and dotted (blue) lines represent the modified PREM, AK135, and PEM-A, respectively.